

## Effect of a high transverse magnetic field on the tunneling through barriers between semiconductors and superlattices

L. Brey

*Departamento de Física de la Materia Condensada, Universidad Autónoma Cantoblanco, 28049 Madrid, Spain*

G. Platero

*Instituto de Ciencia de Materiales, Consejo Superior de Investigaciones Científicas, Universidad Autónoma, Cantoblanco, 28049 Madrid, Spain*

C. Tejedor

*Departamento de Física de la Materia Condensada, Universidad Autónoma, Cantoblanco, 28049 Madrid, Spain*

(Received 2 May 1988)

We present a quantum-mechanical analysis of magnetotunneling in a high transverse magnetic field  $B$ . We use a transfer-Hamiltonian technique for computing the current density through a barrier as a function of both  $B$  and the bias voltage  $V$ . Several systems of the type semiconductor-barrier-semiconductor and superlattice-barrier-superlattice are studied. From our results quantum oscillations and negative differential conductance are interpreted in terms of variations in the available channels for tunneling. Special attention is devoted to the comparison with previously reported experimental information.

### I. INTRODUCTION

The present availability of high magnetic fields and high-quality semiconductor heterostructures grown by molecular-beam epitaxy has allowed an enormous advance in the experimental study of magnetotransport in low-dimensional electronic systems. A great part of such effort has been devoted to the geometrical configuration of the quantum Hall effect where a magnetic field  $B$  is perpendicular to the electronic currents. A closely related problem of increasing interest is the effect of a transverse  $B$  on the tunneling through a barrier separating either two semiconductors<sup>1-4</sup> (SC) or two superlattices<sup>5</sup> (SL). In the case of semiconductors, the current intensity  $I$  for a given bias voltage  $V$  applied to the barrier decreases monotonously for increasing  $B$ .<sup>1,2</sup> Only the second derivative  $d^2I/dB^2$  shows quantum oscillations.<sup>2</sup> For a SL-barrier-SL system negative differential conductance (NDC) regions in the current-voltage characteristics are observed for low magnetic fields, but this feature decreases significantly or even disappears when  $B$  increases.<sup>5</sup> The analysis of these experiments has been performed by means of either a semiclassical WKB approach<sup>1,5</sup> or by qualitative arguments about the magnetic-field effects on the electronic states.<sup>2</sup> A complete understanding of those experiments is not simple because the theoretical effort devoted to magnetotunneling in this configuration is scarce. Magnetotransport in transverse fields has been studied in a semiclassical macroscopic framework<sup>6</sup> by using effective resistance and temperature arguments. Therefore, such a scheme is more concerned with inelastic-scattering processes than with quantum-tunneling effects. Recently, some model

problems within the extreme quantum limit ( $\hbar\omega_c \rightarrow \infty$ ) have been treated by either Landauer-type formulas<sup>7</sup> or by path-integral methods.<sup>8</sup> Apart from this, no quantum-mechanical calculations of tunneling currents in actual systems have been reported.

The aim of this paper is to present a generalization of the transfer-Hamiltonian method<sup>9</sup> for studying tunneling of electrons through a barrier of width  $l_b$  and height  $V_b$  with a bias voltage between two semi-infinite media in the presence of a transverse  $B$ . Each of the two media is in thermal equilibrium but their two chemical potentials are shifted from each other by the bias  $V$  dropping across the barrier. The existence of  $B$  produces important effects both in the electronic spectra and in the tunneling-selection rules that we will analyze in detail. We are concerned with elastic-tunneling effects that in practice are superimposed on the background due to dissipative scattering processes. This method allows us to compute the current density  $j$  as a function of  $V$  and  $B$  obtaining quantum oscillations and NDC features. We will discuss in detail the cases of samples previously studied experimentally as well as others that our calculations indicate to be of potential interest.

The paper is organized as follows. In Sec. II we present the theoretical method used to compute tunneling currents through a barrier. In Sec. III we apply the method to the case of semiconductor-barrier-semiconductor. There, we compare our results with available experimental information and analyze two systems that have not yet been experimentally studied. Section IV is devoted to the SL-barrier-SL system with special emphasis on using our results for understanding the experiments reported previously. Some conclusions and a summary are contained in Sec. V.

## II. METHOD

### A. Stationary states

Before introducing the ingredients that characterize tunneling problems, let us start by sketching the effects of a magnetic field  $B\mathbf{u}_x$  directed along one of the principal axes of a crystal with potential  $U(\mathbf{r})=U(\mathbf{r}+a_x\mathbf{u}_x$

$+a_y\mathbf{u}_y+a_z\mathbf{u}_z)$ . In the gauge  $\mathbf{A}=(0,-Bz,0)$  the Schrödinger equation

$$\left[ \frac{1}{2m}(\mathbf{p}-e\mathbf{A})^2+U(\mathbf{r}) \right] \psi_{\mathbf{k}}(\mathbf{r})=E_{\mathbf{k}}\psi_{\mathbf{k}}(\mathbf{r}) \quad (1)$$

becomes

$$\left\{ \frac{-\hbar^2}{2m} \left[ \left( ik_x + \frac{\partial}{\partial x} \right)^2 + \left( ik_z + \frac{\partial}{\partial z} \right)^2 + \left( ik_y + \frac{ieBz}{\hbar} + \frac{\partial}{\partial y} \right)^2 \right] + U(\mathbf{r}) \right\} u_{\mathbf{k}}(\mathbf{r})=E_{\mathbf{k}}u_{\mathbf{k}}(\mathbf{r}), \quad (2)$$

where we have taken the usual form

$$\psi_{\mathbf{k}}(\mathbf{r})=u_{\mathbf{k}}e^{i\mathbf{k}\cdot\mathbf{r}}. \quad (3)$$

Equation (2) suggests that, in order to recover a generalized Bloch condition,<sup>10,11</sup> one can perform the gauge transformation

$$\mathbf{A} \rightarrow \mathbf{A}e^{-iyeBpa_z/\hbar}, \quad (4)$$

$p$  being an integer number. Then, one has a new periodicity  $\psi_{\mathbf{k}+\mathbf{g}_m}=\psi_{\mathbf{k}}$  with  $\mathbf{g}_m=eBa_z\mathbf{u}_y/\hbar$  superimposed on the crystalline one  $(2\pi/a_y)\mathbf{u}_y$ . In the case in which  $(peBa_z/\hbar)(a_y/2\pi)$  is not an integer number the system presents incommensurability and, consequently, very special properties.<sup>11,12</sup> However, when  $peBa_z a_y/\hbar 2\pi$  is an integer number  $q$ , one recovers a perfectly periodic sys-

tem.<sup>10,11</sup> In many cases,  $a_y$  is much smaller than the magnetic field length  $l_m=\sqrt{\hbar/eB}=256/\sqrt{B}$  Å ( $B$  in teslas) so that  $g_m \ll g_y$ . Then the Hamiltonian can be treated in an effective-mass approximation for the crystal potential  $U(\mathbf{r})$ , being  $\mathbf{g}_m=(a_z/l_m^2)\mathbf{u}_y$ , the only periodicity explicitly appearing in the problem.<sup>13,14</sup> Such approximation is not adequate for a SL where there is a potential  $V_{\text{SL}}(z)$  with a periodicity  $a_z$  comparable with  $l_m$ . Then it is preferable to treat explicitly  $V_{\text{SL}}(z)$  keeping the effective-mass approximation just for the crystal potential of each component of the SL.<sup>13,14</sup> We are interested in extending this scheme to a system where an additional potential breaks some symmetry. In particular, we have a barrier potential  $V_b(z)$  separating two semi-infinite crystals as depicted in Fig. 1. The stationary states of the whole system can be obtained from the Schrödinger equation that in the effective-mass approach described above is

$$\left[ \frac{\hbar^2 k_x^2}{2m_0 m^*(z)} - \frac{\hbar^2}{2m_0} \frac{\partial}{\partial z} \left[ \frac{1}{m^*(z)} \frac{\partial}{\partial z} \right] + \frac{e^2 B^2}{2m_0 m^*(z)} \left( z + \frac{\hbar k_y}{eB} \right)^2 + V_b(z) \right] e^{ik_x x} e^{ik_y y} \phi(z) = E e^{ik_x x} e^{ik_y y} \phi(z), \quad (5)$$

where  $m_0$  is the free-electron mass and the effective mass  $m^*$  is allowed to have different values in the two crystals and in the barrier.<sup>15</sup> The mixing between  $k_y$  and  $z$  as discussed in Eqs. (2) and (4) appears very clear in Eq. (5). Sometimes it is useful for practical purposes to relate the quantum number  $k_y$  with a “center” of the electronic orbit

$$z_0 = \frac{\hbar k_y}{eB} = l_m^2 k_y. \quad (6)$$

In order to make the discussion easier, let us take  $m^*(z)$  as a constant in Eq. (5). Then one obtains

$$E = \frac{\hbar^2 k_x^2}{2m^* m_0} + E_{n,k_y}, \quad (7)$$

where the magnetic levels  $E_{n,k_y}$  must be computed from

$$\left[ -\frac{\hbar^2}{2m^* m_0} \frac{\partial^2}{\partial z^2} + \frac{e^2 B^2}{2m^* m_0} (z+z_0)^2 + V_b(z) - E_{n,k_y} \right] \phi(z) = 0. \quad (8)$$

For a given value of  $k_y$  (or  $z_0$ ) this one-dimensional equation (8) can be solved numerically by means of a finite-elements method.<sup>13</sup> In Fig. 1(b) we show the different curves  $E_{n,k_y}$  obtained in a model problem for clarifying the following discussion. As depicted in the figure, the states at anticrossings between different branches have wave functions shared between the two crystals. The eigenstates away from the anticrossings have wave functions which are only at one of the sides of the barrier. The states at anticrossings form the channels for the magnetotunneling because they allow the electron wave packets initially appearing to the left side pass through the barrier to the right side. The best way for treating such a process is to use a transfer-Hamiltonian technique<sup>9</sup> such as the one we are going to introduce now.

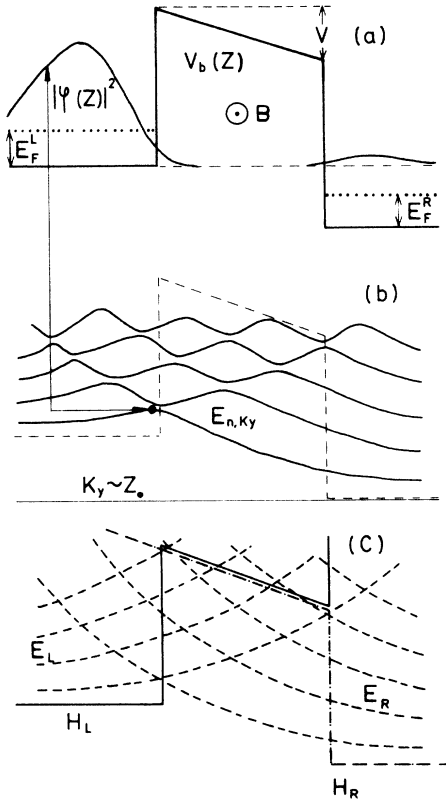


FIG. 1. (a) Potential profile  $V_b(z)$  of a barrier with  $V_b=0.3$  eV,  $l_b=100$  Å, and an applied bias  $V=0.1$  V between two crystals with Fermi levels  $E_F^L$  and  $E_F^R$  (dotted lines). The probability density  $|\phi(z)|^2$  of a magnetic level in the presence of an in-plane magnetic field  $B=10$  T is also shown. (b) Magnetic levels  $E_{n,k_y}$  (solid lines) of the Hamiltonian  $H$  depicted in (a) as a function of  $k_y$  or of its associated orbit "center"  $z_0$ . The dot labels the level for which  $|\phi(z)|^2$  is given in (a). Dashed line gives  $V_b(z_0)$  in order to facilitate the discussion. (c) Model left  $H_L$  (solid line) and right  $H_R$  (dashed-dotted line) Hamiltonians used to compute tunneling current densities in the transfer-Hamiltonian method (see text). Dashed lines depict the magnetic levels for these Hamiltonians including an in-plane magnetic field.

## B. Transfer-Hamiltonian method for magnetotunneling

This method<sup>9</sup> gives a time-dependent formulation of tunneling probabilities. It is based on the separation of the total Hamiltonian in two spacial regions left ( $L$ ) and right ( $R$ ) (see Fig. 1). Then, one writes

$$H = H_L + V_L = H_R + V_R \quad (9)$$

with  $H \equiv H_L$  in the left side and  $H \equiv H_R$  in the right side. Moreover,  $H_L$  and  $H_R$  must be chosen in such a way that their eigenstates  $|L\rangle$  and  $|R\rangle$  are localized in the left and right sides, respectively. The wave functions  $\phi_L(\mathbf{r}) = \langle \mathbf{r} | L \rangle$  and  $\phi_R(\mathbf{r}) = \langle \mathbf{r} | R \rangle$  can be considered as wave packets of the actual problem. Then, tunneling processes are described by a time-dependent perturbation theory which gives the transition probability between an initial state  $\phi_L(\mathbf{r})$  and any possible final state  $\phi_R(\mathbf{r})$  in terms of a kind of Fermi golden rule<sup>9</sup>

$$P_{LR} = \frac{2\pi}{\hbar} |\langle R | V_L | L \rangle|^2 \delta(E_L - E_R). \quad (10)$$

After some manipulation this can be written as

$$P_{LR} = \frac{2\pi}{\hbar} |T_{LR}|^2 \delta(E_L - E_R), \quad (11)$$

where

$$T_{LR} = \frac{-\hbar^2}{2m_0 m^*} \int (\phi_R \nabla \phi_L - \phi_L \nabla \phi_R) \cdot d\mathbf{S}_{LR}, \quad (12)$$

the current being evaluated on the surface  $S_{LR}$  separating the left and right regions. In one dimension, the integral reduces to compute the current at some point in the barrier. The main constriction of this theory is that of being a perturbation method. Then, it is necessary that the spectrum of  $H$  be close to the combination of those  $H_L$  and  $H_R$ .<sup>9</sup> We have checked out this condition by integrating for  $H_L$  and  $H_R$  equations similar to (8). The results are shown in Fig. 1. There, one can see that the dispersion relations of  $H$  [solid lines in Fig. 1(b)] are a perturbation of the dispersion relations of  $H_L$  and  $H_R$  [dashed lines in Fig. 1(c)].

For magnetotunneling in transverse  $B$  the application of Eqs. (10)–(12) simplifies because, as discussed in Sec. II A, the problem is separable. In other words, in Eqs. (10),  $V_L$  is only a function of  $z$  so that both  $k_x$  and  $k_y$  are good quantum numbers which must be conserved in the transition between  $\phi_L(\mathbf{r})$  and  $\phi_R(\mathbf{r})$ , i.e.,

$$T_{LR} \propto \delta(k_y^L - k_y^R) \delta(k_x^L - k_x^R). \quad (13)$$

Then, the practical procedure is as follows: (i) to integrate two one-dimensional equations like Eq. (8) with the potential profiles of  $H_L$  and  $H_R$  [shown in part (c) of Fig. 1], respectively, instead of  $V_b(z)$ ; (ii) to look for the crossing between the two dispersion relations  $E_{n,k_y}^L$  and  $E_{nk_y}^R$ ; and (iii) to evaluate Eqs. (11) and (12) only for the eigenstates corresponding to such crossings.

It must be pointed out that these crossings transform in the anticrossings of the dispersion relation of  $H$  being the only possible tunneling channels as we have men-

tioned in Sec. II A.

Once one can calculate the transition probability from the left to the right of the barrier, the current is computed by considering the occupations of the initial and final states. This requires the calculation of the Fermi level in each medium ( $E_L^F$  and  $E_R^F$ ) in the presence of the magnet-

ic field. This is a bulk property of the two crystals that does not present any special difficulty. From that information, the current density is computed by summing up all the transition probabilities between occupied states to the left and empty states to the right. For zero temperature, we have

$$j = \frac{2e}{(2\pi)^2} \sum_{n,n'} \int dk_x dk_y \frac{2\pi}{\hbar} |T_{LR}(E, k_y)|^2 [\Theta(E_L^F - E_{n,k_y}^L) - \Theta(E_R^F - E_{n',k_y}^R)] \delta(E_{n,k_y}^L - E_{n',k_y}^R), \quad (14)$$

where  $n$  and  $n'$  are indices running over the magnetic levels of  $H_L$  and  $H_R$ , respectively. In Eq. (14) the integral in  $k_x$  is straightforward because for this variable the dispersion relations are simply parabolas. The integral in  $k_y$  is performed using

$$\delta(E_{n,k_y}^L - E_{n',k_y}^R) = \frac{1}{\left| \frac{d(E_{n,k_y}^L - E_{n',k_y}^R)}{dk_y} \right|_{k_y^c}} \delta(k_y - k_y^c), \quad (15)$$

where  $k_y^c$  stands for the crossing  $nn'$ , i.e., the value in which  $E_{n,k_y}^L = E_{n',k_y}^R$ . After some algebra the current density is given by

$$j = \frac{2e(2m_0m^*)^{1/2}}{\pi\hbar^2} \sum_c \frac{|T_{LR}(k_y^c)|^2}{\left| \frac{d(E_n^L - E_{n'}^R)}{dk_y} \right|_{k_y^c}} \{ (E_L^F - E_c)^{1/2} [\Theta(E_L^F - E_c) - \Theta(E_R^F - E_c)] + [(E_L^F - E_c)^{1/2} - (E_R^F - E_c)^{1/2}] [\Theta(E_c) \Theta(E_R^F - E_c)] \}, \quad (16)$$

where the sum runs over all the crossings  $k_y^c$  with energy  $E_c$  discussed above. In (16) the origin of energies is in the bottom of the potential to the left and we have taken the crystal to the right shifted down in  $V$  (as shown in Fig. 1) with respect to the left. To compute the current density  $j$  from Eq. (16) we use  $T_{LR}(k_y^c)$  calculated as discussed above and  $|d(E_n^L - E_{n'}^R)/dk_y|_{k_y^c}$  is also evaluated from the dispersion relations of  $H_L$  and  $H_R$ . It must be pointed out that the current through the barrier in the  $z$  direction is essentially controlled by the dependence on  $k_y$  because the magnetic field associates these two magnitudes as shown in Eq. (6). Once electrons cross the barrier, inelastic processes restore the equilibrium in the right side where  $E_R^F$  is lower than the initial energy of those electrons due to the bias.

### III. SC-BARRIER-SC

In this section we apply the method presented above for analyzing magnetotunneling between two semi-infinite  $n$ -doped GaAs separated by a  $\text{Al}_x\text{Ga}_{1-x}\text{As}$  barrier. The ternary compound forming the barrier has  $x < 0.43$  so that we are concerned with electrons at the bottom of the conduction band in the  $\Gamma$  point. Then, a simple square barrier model of height  $V_b = 0.94x$  eV for electrons with  $m^* = 0.067$  is adequate. Since the semiconductors are  $n$  doped, the applied bias voltage just drops at the barrier.

As far as the barrier width  $l_b$  is concerned, it is convenient to work with values comparable to  $l_m$  which is the magnitude representing the spatial extension of a given state. For fields between 4 and 20 T in which quantum effects can be expected,  $l_m$  varies between 130 and 50 Å. Therefore we start by studying two different GaAs- $\text{Ga}_{0.68}\text{Al}_{0.32}\text{As}$ -GaAs systems at zero temperature.

(i)  $l_b = 50$  Å with a bias  $V = 0.1$  V and a doping  $n = 10^{18}$  cm $^{-3}$  in the GaAs. Our results for this case are shown in Fig. 2.

(ii)  $l_b = 100$  Å with a bias  $V = 0.2$  V and a doping  $n = 10^{18}$  cm $^{-3}$  in the GaAs. Our results for this case are given in Fig. 3.

In order to understand the different contributions to the observed oscillatory dependence, we include in these figures the Fermi-level variation with  $B$  for the bulk of GaAs with the above given carrier density. At low fields the current oscillations are clearly correlated with Fermi-level oscillations while for higher fields very strong oscillations of  $j$  appear independently of the variation of  $E_F$ . This behavior is clearly understood within our formalism. For a fixed value of  $E_F$ , the dependence on  $B$  of the current due to only one crossing between an occupied  $\phi_L$  and an unoccupied  $\phi_R$  is shown in the dashed line in Fig. 3. At low fields there are many crossings between the spectra of  $H_L$  and  $H_R$ . Then there are so many tunneling channels that the different variations with  $B$  tend

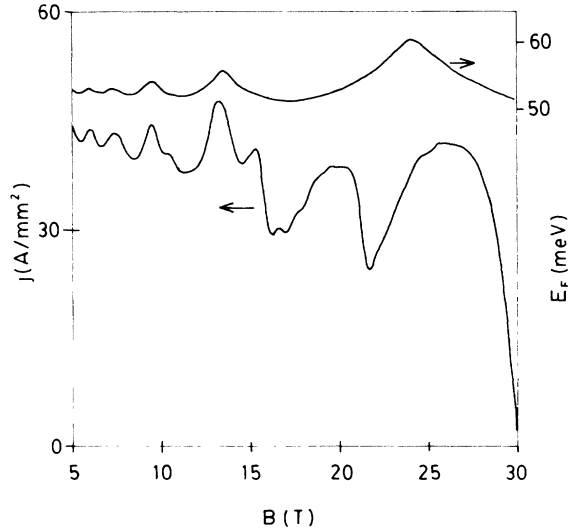


FIG. 2. Current density  $j$  (in  $\text{A}/\text{mm}^2$ ) and bulk GaAs Fermi level (in  $\text{meV}$ ) as a function of an in-plane  $B$  (in teslas) for a GaAs-barrier-GaAs system with  $l_b = 50 \text{ \AA}$ ,  $V_b = 0.3 \text{ eV}$ ,  $V = 0.1 \text{ V}$ , and  $n = 10^{18} \text{ cm}^{-3}$ .

to compensate. Therefore, only bulk oscillations of  $E_F$  reflect in current density oscillations. On the contrary, for higher fields only a few crossings or tunneling channels exist. Then the dependence on  $B$  of each channel (see Fig. 3) clearly reflects in the total  $j$  while  $E_F$  oscillations simply appear as smooth shoulders. An alternative to study these quantum oscillations is to analyze  $j$  as a

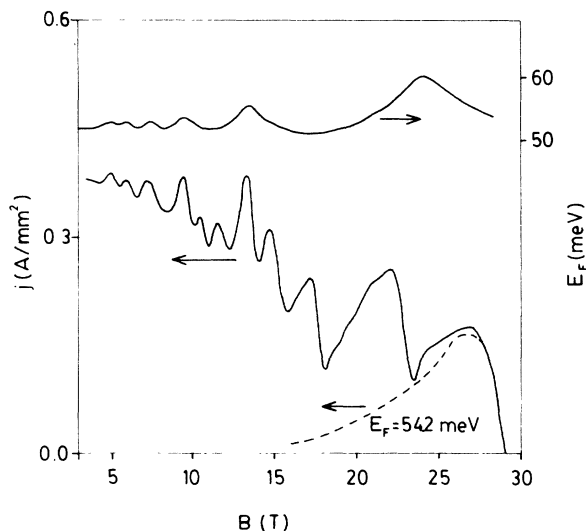


FIG. 3. Current density  $j$  (in  $\text{A}/\text{mm}^2$ ) and bulk GaAs Fermi level (in  $\text{meV}$ ) as a function of an in-plane  $B$  (in teslas) for a GaAs-barrier-GaAs system with  $l_b = 100 \text{ \AA}$ ,  $V_b = 0.3 \text{ eV}$ ,  $V = 0.2 \text{ V}$ , and  $n = 10^{18} \text{ cm}^{-3}$ . Dashed line depicts the current density due to the crossing between the lowest magnetic level of the left Hamiltonian and the lowest of the right one when both GaAs Fermi levels (left and right) are fixed at  $54.2 \text{ meV}$ .

function of the bias  $V$  for a fixed  $B$  because in such a case the Fermi level does not change. The results for the case of  $l_b = 100 \text{ \AA}$  and  $B = 10 \text{ T}$  are shown in Fig. 4. Small oscillations are superimposed on the expected monotonous increase of  $j$  with the bias. Once again the origin of the oscillations is a variation in the number of channels available for tunneling. For this field of  $10 \text{ T}$  in Fig. 4 current flows for very small bias voltage. When  $B$  increases there is a threshold bias to have net tunneling current. This is because for high  $B$  the crossings are so high in energy that a large  $V$  is necessary to get a tunneling channel below  $E_F^L$ .

The main question arising from the results shown in Figs. 2–4 is the possibility of observing experimentally those quantum oscillations. To our knowledge the only reported experiments on this problem are those of Gueret *et al.*<sup>1</sup> They use two different samples formed by two semi-infinite GaAs with a doping of  $n = 10^{17} \text{ cm}^{-3}$  separated by barriers  $l_b = 250 \text{ \AA}$ ,  $V_b = 83 \text{ meV}$ , and  $l_b = 430 \text{ \AA}$ ,  $V_b = 40 \text{ meV}$ , respectively. The barriers are so wide that magnetic fields must be small in order to detect tunneling. Figure 5 shows our results for these two samples. Once again we obtain the same kind of quantum oscillations as in other samples. We plot  $\ln(j)$  as a function of  $B^2$  because that is the scale chosen by Gueret *et al.*<sup>1</sup> A quantitative comparison of our results with experimental data is difficult because the latter are given in terms of the total current intensity which depends on geometrical factors. As expected both theory and experiment show that the tunneling decreases with increasing field in a rather faster way for the sample with  $l_b = 430 \text{ \AA}$  than for the one with  $l_b = 250 \text{ \AA}$ . The main difference is that the oscillations theoretically obtained are not observed in the experimental current intensity. This is probably due to the fact that we only compute elastic tunneling while inelastic-scattering processes introduce a strong background. Therefore, it is just in  $d^2I/dB^2$  where quantum oscillations should appear.<sup>2</sup>

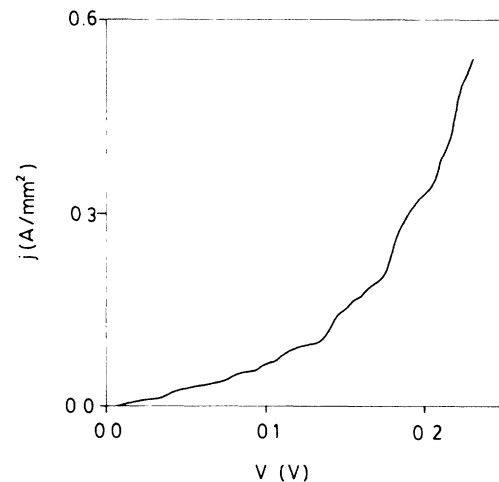


FIG. 4. Current density  $j$  (in  $\text{A}/\text{mm}^2$ ) as a function of the bias voltage  $V$  (in  $\text{V}$ ) for the system of Fig. 3, in a transverse  $B = 10 \text{ T}$  which implies  $E_F = 53.4 \text{ meV}$ .

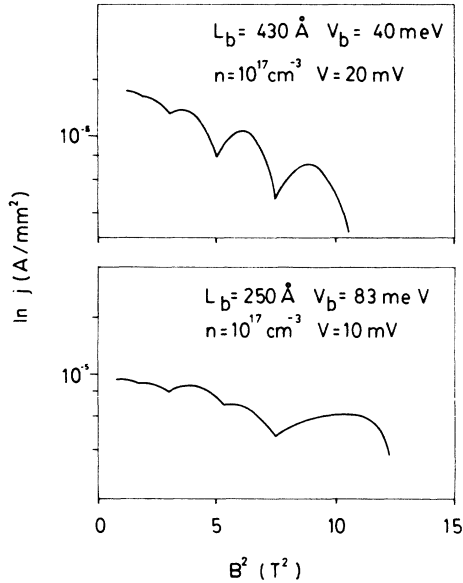


FIG. 5. Logarithm of the current density (in  $\text{A}/\text{mm}^2$ ) as a function of  $B^2$  (in teslas) for the two samples of Gueret *et al.* (Ref. 1) having the characteristics written in the figure.

#### IV. SL-BARRIER-SL

From a fundamental point of view a SL is a perfect crystal so that no essential differences should be expected with respect to the case studied in the previous section. However, as we mentioned in Sec. II, the periodicity of the SL potential  $V_{\text{SL}}(z)$  is comparable to  $l_m$  and new quantum effects are possible. Therefore  $V_{\text{SL}}(z)$  must be explicitly included in Eq. (8) instead of treating it in an effective-mass approach. Apart from this, the method developed here is straightforwardly applicable to compute tunneling current densities in a SL-barrier-SL system.

The anisotropy introduced by  $V_{\text{SL}}(z)$  is the origin of minibands and minigaps in the absence of  $B$ . When a magnetic field  $B\mathbf{u}_x$  exists, the spectrum remembers the minibands because in its energy region the magnetic levels are practically independent of  $k_y$  (flat levels) while in the minigaps regions magnetic levels strongly dependent on  $k_y$  appear.<sup>13,14,16</sup> The two different energy regions are well visualized in the density of states, shown in Fig. 6, obtained from the perfect SL band structure by numerical integration in  $k_x$  and  $k_y$ . Then, for discussion purposes, one can think in minibands and minigaps even in the presence of  $B\mathbf{u}_x$ . As in the case of Sec. III, the magnetic field produces a bending of the dispersion relations for orbit “centers”  $z_0$  close to the interface with the barrier (see Fig. 1). Therefore, tunneling experiments give information on the magnetic levels bent at interfaces instead of doing it on bulk minibands and minigaps.

Davies *et al.*<sup>5</sup> have reported very interesting experiments on transport in the SL-barrier-SL system with a transverse magnetic field. There, it is shown that there are NDC regions that evolve with  $B$  in a similar way for

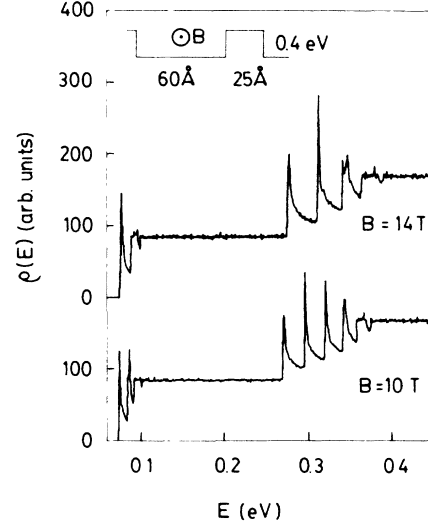


FIG. 6. Density of states  $\rho$  (in arbitrary units) as a function of the energy (in eV) for two different in-plane  $B$  applied to the SL forming part of the sample DB106 of Davies *et al.* (Ref. 5) shown in the inset. The origin of energies is taken at the bottom of the SL wells.

different samples. The general trend is that when  $B$  increases, NDC features move to higher biases and currents. The ratio of the peak-to-valley currents initially increases but in larger fields it begins to decrease and in some cases the NDC is lost for high fields. Davies *et al.*<sup>5</sup> just give qualitative semiclassical arguments for discussing their results but they suggest that a deeper theoretical understanding is required for high fields. We have applied our method to the most interesting cases of Davies *et al.*<sup>5</sup>

(i) Sample MB275.<sup>5</sup> A barrier with  $l_b = 80 \text{ \AA}$  and  $V_b = 235 \text{ meV}$  between two SL with  $n = 4 \times 10^{17} \text{ cm}^{-3}$ , wells of  $55 \text{ \AA}$  of GaAs and barriers of  $35 \text{ \AA}$  of  $\text{Ga}_{0.75}\text{Al}_{0.25}\text{As}$ .

(ii) Sample DB106.<sup>5</sup> A barrier with  $l_b = 40 \text{ \AA}$  and  $V_b = 400 \text{ meV}$  between two media formed each one by a triple well of  $60 \text{ \AA}$  of GaAs with  $n = 5 \times 10^{17} \text{ cm}^{-3}$  and barriers of  $25 \text{ \AA}$  of  $\text{Ga}_{0.57}\text{Al}_{0.43}\text{As}$ .

Figures 7 and 8 show our results of current-voltage characteristics for those two samples with different transverse magnetic fields. In the case of MB275 we plot our results for the magnetic fields reported by Davies *et al.*<sup>5</sup> while in DB 106 we continue the sequence up to much higher fields in order to discuss carefully some interesting features. In both figures we observe that for low fields there are two main peaks separated by a region where no tunneling currents flow. The lower peak corresponds to crossing between occupied magnetic levels coming from the lowest miniband to the left and empty states coming from the lowest miniband to the right. When the bias increases these two energy regions become misaligned and there are no channels available for the tunneling. For higher fields, states from the first miniband to the left and the second to the right start to be coupled and  $j$  increases

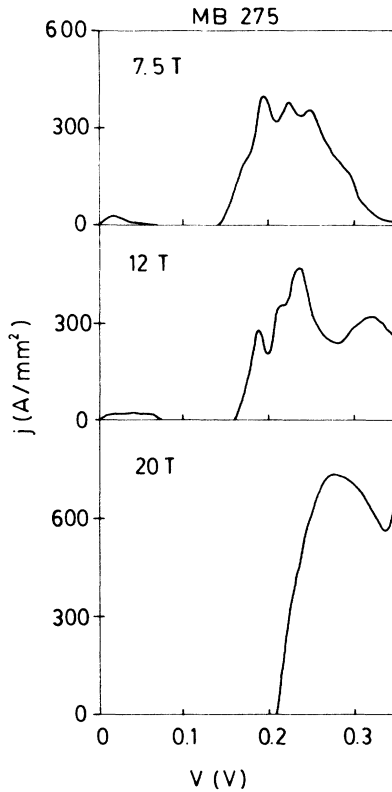


FIG. 7. Current density  $j$  (in A/mm<sup>2</sup>) as a function of the bias voltage  $V$  (in V) for different transverse magnetic fields (in teslas) in the sample MB275 of Davies *et al.* (Ref. 5) (see text).

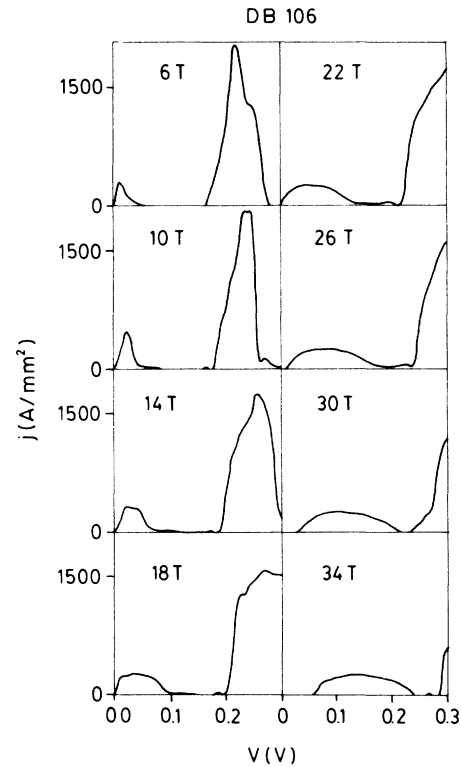


FIG. 8. Current density  $j$  (in A/mm<sup>2</sup>) as a function of the bias voltage  $V$  (in V) for different transverse magnetic fields (in teslas) in the sample DB106 of Davies *et al.* (Ref. 5) (see text).

again. Therefore the bias voltages giving NDC give information on the first minigap. We must insist that around the SL-barrier interface there is an additional bending (see Fig. 1) of the dispersion relations which slightly alters their shape.

The comparison with experiments must be done remembering that, as in the case of GaAs-barrier-GaAs, the elastic-tunneling current is superimposed on a background produced by inelastic-scattering processes. However, the main experimental features are due to elastic tunneling. For small fields, the first peak of  $j$  increases with  $B$  as can be seen in the evolution between 6 and 10 T for sample DB106 (Fig. 8). This is consistent with the experimental increase of the ratio of the peak-to-valley currents. The subsequent experimental decrease of that ratio until the disappearance of NDC is just the lowering of the first peak of  $j$  observed in Figs. 7 and 8. At the same time all the structure of  $j$  spreads and shifts to the right as is experimentally observed. That is due to the fact that higher  $B$  implies a higher energy of the crossings, (i.e., higher bending of the magnetic levels), so that a higher bias is required to get current. In some cases (between 22 and 26 T for DB 106) the first and second minibands slightly overlap. This is due to a different bending of both structures at the interface. The last feature to be pointed out is the appearance in both samples of a threshold bias which increases with  $B$ . Once

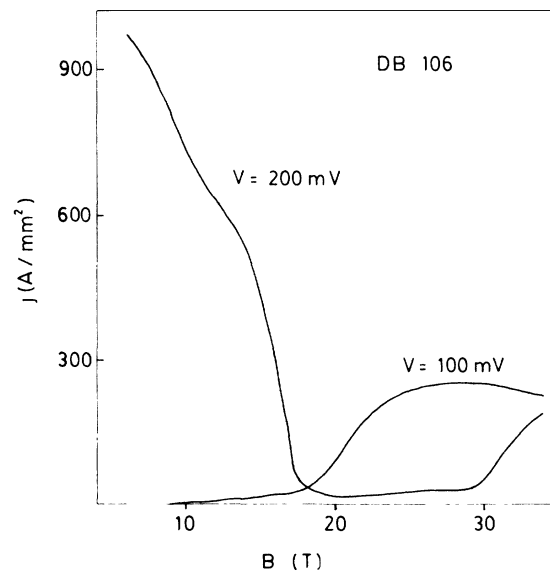


FIG. 9. Current density  $j$  (in A/mm<sup>2</sup>) as a function of the transverse magnetic field (in teslas) for two different bias voltages (in mV) applied to the sample DB106 of Davies *et al.* (Ref. 5) (see text).

again this is caused by the moving up in energy of the tunneling channels as mentioned above. The oscillations superimposed on the main peaks have the same origin as the one observed in the case of GaAs-barrier-GaAs, i.e., the disappearance of a given tunneling channel when there are only a few of them. All the characteristics hitherto discussed manifest in the same way if one represents  $j$  as a function of  $B$  for a given bias as we did for GaAs-barrier-GaAs. The results are shown in Fig. 9 where one observes regions with low current density related to NDC of Fig. 8. We must stress that the narrowness of the minibands implies a rather high density of states for any  $B$ . Therefore the oscillations of the Fermi level when  $B$  varies are much smaller than in the case of GaAs. So the whole structure observed in Fig. 9 is due to changes in the available tunneling channels.

Apart from the inelastic background, the only discrepancy between our results and those of Davies *et al.*<sup>5</sup> is that the experimental features occur at values of  $V$  higher than the theoretical ones. We think that this is due to the fact that the doping of the SL is only within the wells so that the external bias does not drop just in the barrier. Therefore any experimental value of  $V$  corresponds, in fact, to a smaller value of the bias at the barrier improving the agreement with the theory.

## V. SUMMARY AND CONCLUSIONS

The use of a magnetic field has given excellent results to get insight on the electronic structure of a SL grown along a direction perpendicular to the field.<sup>13</sup> Magneto-optics<sup>14,16</sup> has been the technique mainly used for such purpose. Tunneling measurements are an excellent candidate to study the electronic properties of the interfaces of both semiconductors or SL with some other medium. Scarce attempts have been made<sup>1-5</sup> to use transverse magnetotransport to analyze magnetic levels at interfaces. On top of experimental difficulties a quantum theory for this problem was not developed hitherto. In this paper we have presented a transfer-Hamiltonian ap-

proach<sup>9</sup> for computing elastic-tunneling currents in the presence of a magnetic field parallel to the interfaces. The total Hamiltonian is separated in two spatial regions (left and right) and the use of time-dependent perturbation theory gives the transition probability of electrons from one region to the other. The method is conceptually simple and manageable from the numerical point of view. We have used this technique to compute current densities produced by a bias applied either to GaAs-barrier-GaAs and SL-barrier-SL systems. The agreement between our results and experimental ones can be considered satisfactory mainly in the latter case. Some difficulties for a detailed quantitative comparison exist due to the experimental background coming from inelastic scattering mechanisms which are not included in our method. In spite of such difficulty our theoretical scheme allows a better understanding of the experimental data. Using our theoretical results one can identify the origin of any feature as coming from one of the different tunneling channels well individualized in the calculation. The results obtained here encourage us to extend the method to similar problems, as the magnetotunneling through a double barrier where resonance effects can be expected. This is the target of our current work.

*Note added in proof.* After this manuscript was accepted for publication, we became aware of a paper by T. W. Hickmott [Solid State Commun. **63**, 371 (1987)] where the oscillations of the current here obtained were observed experimentally.

## ACKNOWLEDGMENTS

We are indebted to Dr. J. C. Maan for helpful discussions and providing us with a program to solve differential equations by means of a finite-element method. We acknowledge Professor F. Flores for fruitful discussions. This work has been supported in part by the Comision Asesora de Investigacion Cientifica y Tecnica of Spain.

<sup>1</sup>P. Gueret, A. Baratoff, and E. Marclay, *Europhys. Lett.* **3**, 367 (1987).  
<sup>2</sup>B. R. Snell, K. S. Chan, F. W. Sheard, L. Eaves, G. A. Toombs, D. K. Maude, J. C. Portal, S. J. Bass, P. Claxton, G. Hill, and M. A. Pate, *Phys. Rev. Lett.* **59**, 2806 (1987).  
<sup>3</sup>U. Kunze, *Surf. Sci.* **196**, 374 (1988).  
<sup>4</sup>H. Bando, T. Nakagawa, H. Tokumoto, K. Ohta, and K. Kajimura (unpublished).  
<sup>5</sup>R. A. Davies, D. J. Newson, T. G. Powell, M. J. Kelly, and H. W. Myron, *Semicond. Sci. Technol.* **2**, 61 (1987).  
<sup>6</sup>B. Movaghar, *Semicond. Sci. Technol.* **2**, 185 (1987); B. Movaghar, J. Leo, and A. McKinnon (unpublished).  
<sup>7</sup>P. Streda, J. Kucera, and A. H. MacDonald, *Phys. Rev. Lett.* **59**, 1973 (1987).  
<sup>8</sup>J. K. Jain and S. Kivelson, *Phys. Rev. B* **37**, 4111 (1988); **37**, 4276 (1988).  
<sup>9</sup>C. B. Duke, *Tunneling in Solids*, Suppl. 10 of *Solid State Phys-*

*ics* (Academic, New York, 1969).  
<sup>10</sup>W. Y. Hsu and L. M. Falicov, *Phys. Rev. B* **13**, 1595 (1976); D. R. Hofstadter, *ibid.* **14**, 2239 (1976).  
<sup>11</sup>D. J. Thouless, M. Kohmoto, M. P. Nightingale, and M. den Nijs, *Phys. Rev. Lett.* **49**, 405 (1982).  
<sup>12</sup>J. B. Sokoloff, *Phys. Rep.* **126**, 189 (1985).  
<sup>13</sup>J. C. Maan, in *Two-Dimensional Systems Heterostructures and Superlattices*, edited by G. Bauer, F. Kuchar, and H. Heinrich (Springer-Verlag, Berlin, 1984); in *Festkörperprobleme (Advances in Solid State Physics)*, edited by O. Madelung (Pergamon, New York, 1987), Vol. 27, p. 137.  
<sup>14</sup>G. Belle, J. C. Maan, and G. Weimann, *Solid State Commun.* **56**, 65 (1985).  
<sup>15</sup>R. A. Morrow and K. R. Brownstein, *Phys. Rev. B* **30**, 678 (1984).  
<sup>16</sup>T. Duffield, R. Bhat, M. Koza, F. De Rosa, K. M. Rush, and S. J. Allen, Jr., *Phys. Rev. Lett.* **23**, 2693 (1987).